Colloid Polym Sci 279:887–897 (2001)

ORIGINAL CONTRIBUTION

B. S. Huang
L. L. Chang
E. M. Woo

Analysis of dual melting behavior in cold-crystallized poly(ether diphenyl ether metaketone)

Received: 9 January 2001
Accepted: 3 February 2001

B. S. Huang · L. L. Chang
E. M. Woo (✉)
Department of Chemical Engineering
National Cheng Kung University
Tainan 701-01, Taiwan
e-mail: emwoo@mail.ncku.edu.tw
Tel.: +886-6-2757575 ext. 62670
Fax: +886-6-2344496

Abstract By focusing on cold-crystallized poly(ether diphenyl ether metaketone) (PEKm), a more in-depth understanding of the nature of the crystalline morphology has been gained, which may lead to thorough mechanisms for interpreting the observed thermal behavior in PEKm. Apparently, cold-crystallized PEKm containing initially only a single P1 crystal can exhibit dual melting peaks (300 and 320 °C), with the second high-melting peak corresponding to the P2 crystal that was subsequently formed via P1 melting/repacking during the scan. However, dual morphism (preexisting P1 and P2 crystals) could be intentionally introduced into PEKm if it was cold-crystallized at temperature schemes of decreasing order. The P1 and P2 crystals possess the same unit cells (orthorhombic) and thus they differ only in the lamellae populations. The dual lamellar morphism in this PEKm sample also exhibited similar dual melting peaks during scanning, which correspond to melting of the individual P1 and P2 in a sequential order. This study has thus provided important clues in and shed new light on the interpretation of multiple melting with respect to polymorphism in polymers. Relationships between the low-melting and high-melting lamellae in cold-crystallized polyketone polymer have been thoroughly explored.

Key words Poly(ether diphenyl ether metaketone) · Cold crystallization · Polymorphism · Multiple melting

Introduction

Crystalline morphology in poly(aryl ether ketones)-type polymers is a subject of many studies. Ordered structure and processing-related crystalline morphology influence the physical and mechanical properties. The most studied in this class is poly(ether ether ketone), which draws considerable interest owing to its broad applications. Newer variants of this class which contain metaphenyl ketones and/or biphenylether in the chain backbones have been synthesized. The unusual melting and crystallization of this type of polymer have been reported and various interpretations have been offered [1, 2, 3]. The thermal behavior and the crystalline morphology in certain semicrystalline polymers are complex and the polymers usually exhibit double melting or multiple melting peaks, in addition to a typical "annealing peak" that is located 10–20 °C above the temperature at which the polymers are isothermally crystallized or annealed. Confusion owing to the complexity in the crystalline morphology has also been encountered in polyketone-type polymers. Various interpretations include mechanisms of reorganization or melting/recrystallization (upon scanning or annealing) [4, 5, 6], different lamellar morphologies [2, 7], or simultaneous existence of different crystal entities [8, 9]. The melting/recrystallization mechanism coupled with the polymorphism of different unit-cell crystals could lead to more complex thermal behavior, as recently demonstrated in syndiotactic polystyrene

showing four sharp melting peaks with two different unit cells [10].

Multiple melting and morphology in polyketone polymers have been confusing and lack consistent agreement on the interpretations. Our concurrent studies as well as a few other reports [11, 12, 13, 14] have investigated melt-crystallized poly(ether diphenyl ether metaketone) (PEKm) as independent and separate scopes in order to examine the relationships between morphology and thermal behavior in polyketone polymers from a wide variety of perspectives. The thermal behavior and morphology are quite different between cold-crystallized and melt-crystallized PEKm. This study focused on probing the behavior of the polymer as it formed crystals from a quenched amorphous glassy polymer. The main objective of this study concerned the elucidation of the crystal and/or lamellar morphology in cold-crystallized PEKm. By carefully designing thermal treatments on samples, the morphology and thermal characterization were performed on PEKm that had been subjected to specific thermal histories. By extending the studies from a focus on the melt-crystallized morphology to the cold-crystallized one, it was expected to reach a more in-depth understanding of the nature of the crystalline morphology that may lead to the observed thermal behavior in PEKm. Especially, mechanisms were examined to confirm routes via repacking of higher-melting crystals by melting/recrystallizing previously existing lower-melting crystals. Alternative mechanisms via different routes were also checked. Relationships between the low-melting and high-melting crystals in cold-crystallized polyketone polymer were investigated and discussed.

Experimental

Materials and preparation

The synthesis of PEKm (or PK99) followed a similar procedure to that reported earlier in the literature [15]; it is stated here briefly. 1,3-Bis(4-flurobenzoyl)benzene was first prepared by a Friedel–Crafts reaction between flurobenzene and isophthaloyl chloride. Then, 1,3-bis(4-flurobenzoyl)benzene (3.223 g or 0.01 mol), 4,4-dihydroxybiphenyl (1.862 g or 0.01 mol), and diphenylsulfone (7.80 g) solvent were charged into a four-neck flat-bottomed flask fitted with a stirrer, a condenser, and a nitrogen inlet. The mixture in the flask was first heated in a sand bath to 175 °C. Sodium carbonate (1.06 g or 0.01 mol) and potassium carbonate (0.028 g or 0.0002 mol) were added as catalysts. The temperature was raised slowly to 300 °C and maintained for 10 min. An additional quantity of 1,3-bis(4-flurobenzoyl)benzene (0.02 g) was introduced into the flask. The mixtures were allowed to react for a further 5 min, then the product was poured onto an aluminum sheet, cooled and ground to a powder. The diphenylsulphone solvent and residual salts in the product were removed by leaching repeatedly (several times), first with 200 ml acetone (20 °C), and then with water (80 °C). The polymer was dried at 120 °C under vacuum. The final yield (after leaching and purification) was found to be 85%. T_g was found to be 155 °C (onset) and the apparent T_m was 308 °C (peak position), in general agreement with the literature values. The chemical structure is shown as follows:

For preparing cold-crystallized samples, initially amorphous PEKm was needed as a starting material. Amorphous PEKm (free of initial crystallinity) could be obtained by heating the synthesized polymer to 340 °C, compression-molded into a thin film (between two aluminum plate molds), then quenched quickly into liquid nitrogen or ice–water. Transparent, crystal-free, amorphous material was obtained upon quenching. The amorphous film was then cut into discs of proper sizes for various thermal treatments (cold crystallization at designated temperatures for various times). For exact temperature accuracy, all thermal treatments of the samples were performed in the precision-temperature cells of the differential scanning calorimeter (DSC). After thermal treatments had been properly done in the DSC, the samples were ready for X-ray diffraction or optical microscopy characterization.

Apparatus

Thermal characterization (crystallization and melting) of the samples was performed using a DSC(Perkin-Elmer DSC-7) equipped with an intracooler and a computer for data acquisition/analysis. For various sensitivity/resolution combinations, various heating rates were used as necessary. Typical scan rates were 2, 5, 10, 20, and 40 °C/min. The peak temperatures and the enthalpy of crystallization/melting were measured at scan rates as specified in the figures or the text, unless otherwise indicated. The calorimetric measurements were performed immediately after the polymer samples had been quenched in the DSC cells from their molten state.

The unit-cell packing in the cold-crystallized PEKm samples was characterized using an X-ray instrument (Rigaku D/Max II-B) with Cu Kα radiation ($\lambda = 0.1542$ nm). For a direct comparison with the DSC results, the specimens for X-ray characterization were prepared using the same thermal treatments as described for the thermal analysis samples. A polarized-light optical microscope (Nikon Optiphot-2 POL) with a microscope heating stage (Linkam THMS-600 with TP-92 temperature programmer) was used to examine the spherulite structure and/or growth rates. Thin films of polymer samples (originally quenched amorphous glass) were deposited on glass slides. Subsequently, desired thermal treatments were performed on the programmed heating stage.

Results and discussion

Multiple crystallization and melting in PEKm

The crystallization from the amorphous rubbery state the and subsequent thermal transitions of PEKm and their relationships with the crystalline morphology developed were investigated first. The quenched amorphous glassy samples of PEKm were scanned in the DSC from 75 to 340 °C at heating rates ranging from 2 to 20 °C/min. The DSC results of different scanning rates are summarized in Fig. 1. When scanned at lower heating rates (e.g., 10, 5, and 2 °C/min, respectively), the samples exhibited multiple (2–3) crystallization exotherms (labeled $T_{c,1}$, $T_{c,2}$, and $T_{c,3}$) and two melting peaks (labeled P1 and P2, with $T_{m,1} = 301$ °C, $T_{m,2} = 323$ °C when scanned at 2 °C/min). The third crystallization exotherm ($T_{c,3}$) can be revealed only when PEKm is scanned in the DSC at low rates (e.g.,

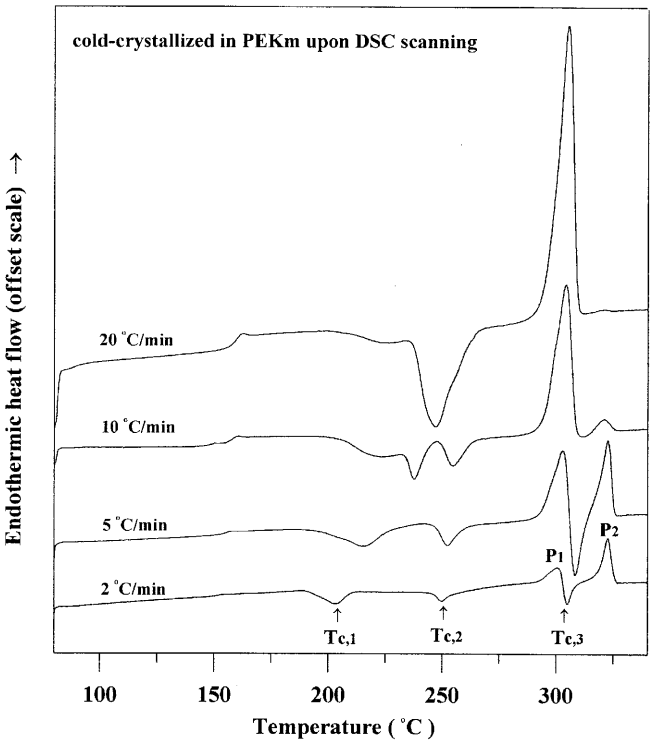

Fig. 1 Differential scanning calorimeter (*DSC*) analyses of different scanning rates on cold-crystallized poly(ether diphenyl ether metaketone) (*PEKm*)

2 or 5 °C/min), and it is located between the P1 and P2 melting peaks. However, DSC scanning at the higher rate of 20 °C/min revealed only a crystallization peak (245 °C), which apparently is a merged exotherm of the $T_{c,1}$ and $T_{c,2}$ peaks, and a melting peak (P1 at 302 °C) with P2 absent.

We discuss the crystallization peaks first. Depending on the scanning rates, the crystallization peaks were found at slightly different temperatures. For the DSC thermogram (2 °C/min), three crystallization exotherms are located at 201, 250, and 304 °C, respectively. At higher scanning rates, the first crystallization peak ($T_{c,1}$) moves to a gradually higher temperature. The second crystallization exotherm also increases slightly with heating rate; but the increase in the peak position with the DSC scanning rate for the second crystallization peak ($T_{c,2}$) is much less than for the first one ($T_{c,1}$). Thus, for samples scanned at 20 °C/min, the first and second crystallization exotherms are superimposed and merged to one (near 245 °C), while the third crystallization peak is diminished to an insignificant amount. The quantitative values of the thermal characteristics of cold crystallization in an originally amorphous/quenched PEKm when scanned in the DSC at various heating rates are listed in Table 1. An apparent trend can be observed in that the enthalpy ratio related to the relative magnitude of P1 and P1, i.e., $\Delta H_{f,1}/\Delta H_{f,2}$, rapidly decreases to zero with the increasing DSC scan rate. This clearly suggests that the P2 crystal (lamellae) may be grown only after P1 has melted and the sample is brought (scanned) to a higher temperature. Higher scanning rates are unfavorable for such a process. The number of P2 crystal entities that can be grown during scanning is dependent on the heating rate.

Thus, the thermal behavior and morphology of cold-crystallized PEKm seems to be quite complex. The last result (scanned at 20 °C/min), showing a single crystallization exotherm and a single melting peak in PEKm, is in agreement with that obtained by Blundell et al. [2]; however, the behavior of multiple crystallization and the melting peaks as revealed by using lower scanning rates have yet to be explained. The reduction and eventual disappearance of the third crystallization exotherm (at 305 °C when scanned at 2 °C/min) with increasing heating rates (e.g., 20 °C/min or greater) is believed to be associated with insufficient time of recrystallization at higher scanning rates and will be expounded more with further evidence. When PEKm was heated to 340 °C (above its apparent melting point), it turned into a liquid state. As the polymer liquid was cooled from liquid state (340 °C) to 100 °C at −10 °C/min, it exhibited a single crystallization exotherm peak at about 260 °C ($\Delta H_c = -52$ J/g). For brevity, the DSC traces for the cooling process are not shown. The slowly cooled and solidified PEKm sample was then scanned up from 100 to 340 °C at 10 °C/min, and three melting peaks were revealed in the sample. The first peak is a partially merged doublet endotherm and is located near 303 °C, with the minor shoulder peak at about 299 °C. The

Table 1 Thermal characteristics of cold-crystallized of poly(ether diphenyl ether metaketone) (*PEKm*) using a differential scanning calorimeter (*DSC*) at various scanning rate. $\Delta H_{c,3}$ is the heat of the third crystallization peak (the recrystallization exotherm that takes place between the P1 and P2 melting peaks)

Scan rate (°C/min)	$T_{m,1}$ (°C)	$T_{m,2}$ (°C)	$\Delta H_{f,1}$ (J/g)	$\Delta H_{f,2}$ (J/g)	$\Delta H_{c,3}$ (J/g)	$\Delta H_{f,2}/\Delta H_{f,1}$
2	300.58	322.73	23.02	50.17	−16.5	2.3
5	302.98	322.72	43.92	35.33	−22.0	0.82
10	304.33	321.25	51.50	3.0	−0.002	0.06
20	305.31	–	51.53	0	0	0

collective heat of fusion (ΔH_f) for the first doublet endotherm is 52 J/g, which is about the same (in magnitude) as the crystallization exotherm released during the cooling from the melt state. The estimated enthalpy of fusion for fully crystalline PEKm is about 125.0 J/g [2]. The second melting endotherm, smaller and located at a higher temperature of about 322 °C, is completely resolved and separate from the first melting peak.

The result of DSC scanning at 20 °C/min is in good agreement with Blundell et al. [2], who reported that only PEKm postannealed at 310 °C would show two melting peaks (308 and 318 °C, respectively); however, the DSC result in this study showed that dual melting behavior was present in the samples regardless of postannealing at 310 °C. The results in Fig. 1 show that the high-melting peak (P2) could be observed in any quenched amorphous samples upon scanning as long as the heating rates were not too fast (e.g., below 20 °C/min). The P2 crystal entity could apparently be generated upon dynamic scanning of the originally amorphous PEKm in addition to postcrystallization annealing at the isothermal temperature of 310 °C. While annealing of the samples at 310 °C might further change the relative numbers of crystal entities responsible for these two melting exotherms, a dual melting phenomenon could actually be seen in the quenched amorphous PEKm upon scanning at slow enough rates (e.g., 10 °C/min or lower). However, it must be understood exactly how the crystal entities of P1 and P2 are related, and under what circumstances the P2 crystal entity could be formed more favorably. With these observations, we proceeded to investigate the origin of these two melting peaks. The crystal entities generated during heating the originally amorphous glassy PEKm have to be analyzed to understand how they are associated with the observed multiple melting peaks. Furthermore, the multiple crystallization peaks demanded more detailed elucidation.

Cold crystallization at $T_{c,1}$ or $T_{c,2}$

We first investigated what difference there might be in the samples if the cold crystallization took place at 230 or 250 °C, which are peak temperatures for the first and second cold-crystallization exotherms ($T_{c,1}$ or $T_{c,2}$, respectively, when quenched samples were scanned at 10 °C/min). The effects of holding time and temperatures were examined. Two sets of samples were isothermally cold-crystallized at 230 or 250 °C, respectively, for times of 10, 30, 45, or 60 min. The crystallized samples were then all scanned in the DSC from the respective holding temperature (230 or 250 °C) at the same heating rate of 10 °C/min.

230 °C-cold-crystallized samples

The DSC results of 230 °C-crystallized samples for various times (10, 30, 45, 60 min) as specified in the thermograms (10 °C/min) are shown in Fig. 2. All thermograms reveal only a cold-crystallization peak (about 260 °C) of about the same magnitude and at the same temperature location. This exotherm apparently corresponds to the second crystallization peak ($T_{c,2}$). It indicates that the cold crystallization for various length of time at 230 °C is responsible for one type of molecular packing, which does not influence or interfere with another type of molecular packing that is yet to take place at the higher temperature of 250 °C. The melting behavior, however, is different depending on the time of crystallization at 230 °C. Dual melting peaks (P1 and P2) are seen in all the thermograms, with one being at about 303 °C and the other at about 322 °C (for samples scanned at 10 °C/min). This is in agreement with the quenched amorphous samples scanned at 10 °C/min, shown in Fig. 1. However, the intensity of the second melting peak decreases with the time of cold crystallization at 230 °C. The result suggests that the cold crystallization at 230 °C may influence the amount of crystal entity that would be available for melting at 323 °C. We elucidate more on this later.

Note that a minor shoulder peak (about 295 °C) is partially merged to the lower-temperature side of P1,

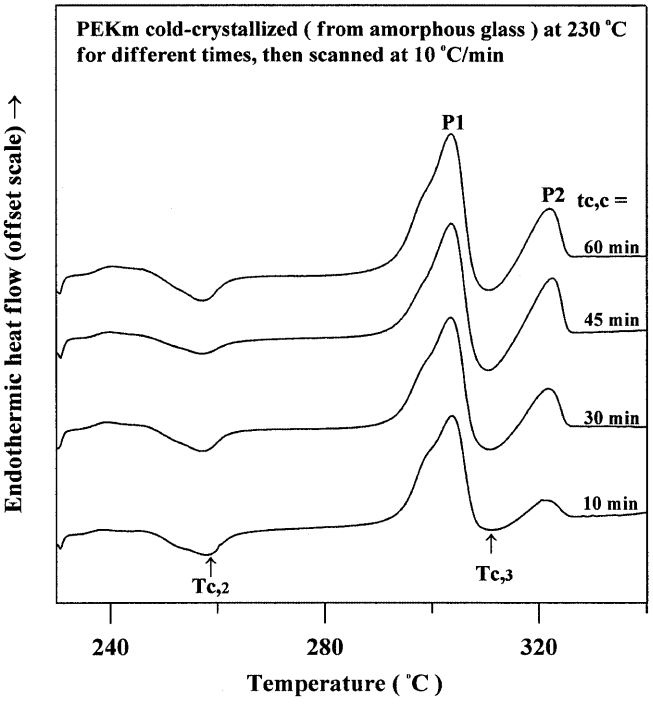

Fig. 2 DSC results of 230 °C-crystallized samples for various times (10, 30, 45, 60 min) as specified in the thermograms (10 °C/min)

and this shoulder peak should not be confused with the conventional annealing peak (usually located 10–20 °C above the crystallization temperature). The shoulder peak can be more noticeable under some circumstances to be discussed later. The origin of this shoulder peak may be attributed to melting of the thinnest lamellae crystals produced during crystallization. For practical reasons, it may be regarded as part of the P1 crystal. The relationship between the lower-melting P1 crystal and the thicker crystal entity of P2 is elucidated in more detail later.

To further understand the relationship between P1 and P2, samples were cold-crystallized (at 230 or 250 °C for 10 min) to develop a fixed amount of crystal entity. They were then scanned in the DSC directly from the holding temperature using a series of different scanning rates from 5 to 40 °C/min. Note that the annealed samples were not quenched to ambient temperatures and were scanned from ambient temperature in order to minimize any further complication of crystal formation or melting during scanning. The DSC traces of 230 °C-crystallized (for 10 min) samples scanned at 5, 10, 20, or 40 °C/min, respectively, are shown in Fig. 3. For all samples, a crystallization exotherm at 260 °C ($T_{c,2}$) is observed and it is also followed by a broad melting endotherm at 240–250 °C. The origin of the broad endotherm at 240–250 °C is apparently associated with melting of some of the thinnest crystal lamellae developed during the previous 230 °C crystallization. Both thermal signals (melting and crystallization between 240 and 260 °C) are obviously enhanced with greater heating rates. In addition to the increased signal intensity, the peak temperature of the second crystallization ($T_{c,2}$) also increases with the heating rate. Furthermore, the signal of P1 (first melting peak) as well as its peak temperature ($T_{m,1}$) is also enhanced with higher heating rates. However, the opposite trend is seen with the third crystallization at 308 °C ($T_{c,3}$) and the second melting peak (P2). The crystallization exotherm and the high-melting peak (P2) were not detected for scanning rates equal to or greater than 20 °C/min. Furthermore, the observed peak temperature of the high-melting peak ($T_{m,2}$) apparently decreases with scanning rate. The variation trends (with scanning rates) are apparently opposite for P1 and P2.

250 °C-cold-crystallized PEKm

Similarly, the DSC scanning (10 °C/min) on 250 °C-crystallized PEKm samples for various times as specified in the curves is shown in Fig. 4. In contrast to the 230 °C-crystallized samples, these 250 °C-crystallized samples did not exhibit the second cold-crystallization exotherm (250 and 260 °C). The melting behavior, however, is different from those cold-crystallized at 230 °C. Similar dual melting peaks (303 and 322 °C) are

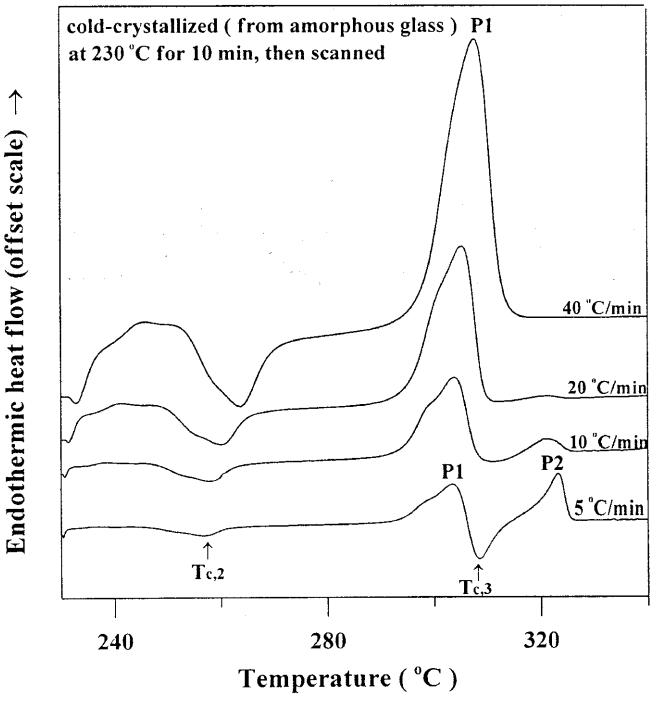

Fig. 3 DSC traces of 230 °C-crystallized (for 10 min) samples scanned at 5, 10, 20, and 40 °C/min, respectively

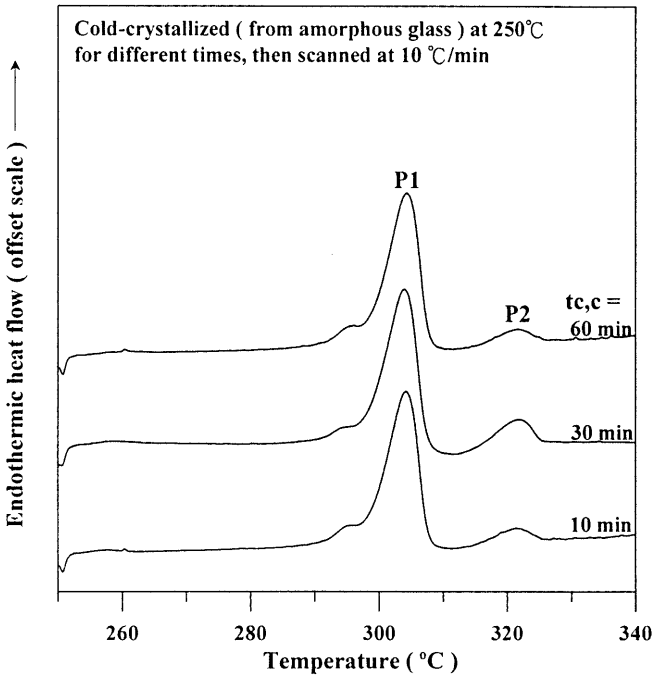

Fig. 4 DSC scanning (10 °C/min) on 250 °C-crystallized PEKm samples for various times as specified in the curves

seen in all DSC thermograms. However, the intensity (heat of fusion) of the second melting peak (about 322 °C) is much smaller than those found in the 230 °C-crystallized samples (shown in Fig. 2); furthermore, the intensity of the second melting peak does not change much with the time of cold crystallization at 250 °C. The result clearly suggests that the cold crystallization at 250 °C has reduced the number of polymer chains available later for packing into a crystal entity that would melt at 323 °C. Further evidence will be discussed in later sections to elucidate how crystallization at 250 °C might lead to a decrease in the crystal entity associated with the melting at 323 °C (P2). In addition, a similar shoulder minor peak (295–300 °C) is located to the underside of P1; however, the shoulder peak for the 250 °C-crystallized samples is merged much more with P1 than that for the 230 °C-crystallized ones. Again, it provides evidence that cold crystallization at the higher temperature of 250 °C reduced the amount of thinnest lamellae associated with the shoulder melting.

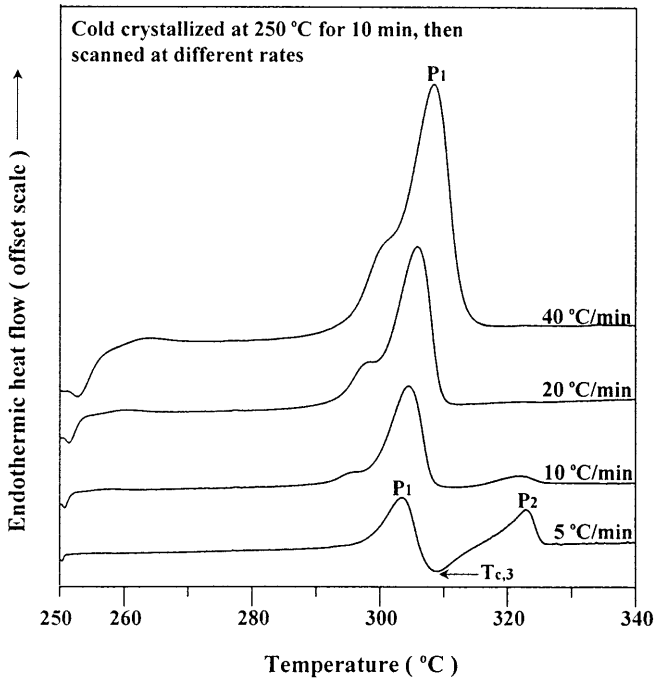

Fig. 5 DSC traces of 250 °C-crystallized (for 10 min) samples scanned at 5, 10, 20, and 40 °C/min, respectively

The DSC traces of 250 °C-crystallized (for 10 min) samples scanned at 5, 10, 20, and 40 °C/min, respectively, are shown in Fig. 5. For all samples, no crystallization exotherms between 200 and 260 °C were observed, suggesting completion of crystallization. This behavior for the PEKm samples cold-crystallized at 250 °C is different from the samples crystallized at 230 °C. The ratio of the signal of P1 (first melting peak) to the signal of P2 is seen to rapidly decrease with higher DSC scanning rates. Lower scanning rates (e.g., 5 °C/min) revealed P1 and P2 with a recrystallization exotherm at 308 °C (i.e., $T_{c,3}$). For DSC scanning rates equal to or greater than 20 °C/min, the recrystallization exotherm ($T_{c,3}$) and the high-melting peak (P2) were not detected. This trend is consistent with that observed in the PEKm samples cold-crystallized at 230 °C.

For quantitative examination, the numerical values of certain critical thermal transitions as observed in 230 °C- and 250 °C-cold-crystallized samples are summarized in Tables 2 and 3, which list the values of $\Delta H_{f,1}$, $\Delta H_{f,2}$, and $\Delta H_{c,3}$ and peak temperatures of the results shown in Figs. 1, 2, 3, and 4. For all the samples, the sums of $\Delta H_{f,1,} + \Delta H_c + \Delta H_{f,2}$ are about the same, except for the samples scanned at high rates (20 °C/min or higher). The almost constant sum suggests that the three thermal processes, i.e., melting of P1, recrystallization of P1 species into P2, and melting of P2, are interrelated, and that if given enough time (e.g., slow scanning rates or holding at temperatures suitable for melted P1 to repack to P2), the melted P1 species (lower melting) can be regained as P2 crystals (higher melting) via recrystallizing the melted P1 polymer chains. These two opposite trends of enthalpy associated with P1 and P2 clearly indicate that the melting of the P2 crystal

Table 2 Summary of main characteristics of P_1 and P_2 in cold-crystallized PEKm samples scanned in a DSC at various rates. All samples were cold-crystallized at 230 or 250 °C for 10 min prior to DSC scanning analysis

Cold crystallization	Scan rate (°C/min)	$T_{m,1}$ (°C)	$T_{m,2}$ (°C)	$\Delta H_{f,1}$ (J/g)	$\Delta H_{c,3}$ (J/g)	$\Delta H_{f,2}$ (J/g)	$\Delta H_{f,2}/\Delta H_{f,1}$
$T_{c,c}$ = 230 °C, 10 min	5	303.5	323	44.5	−25.6	36.1	0.81
	10	303.7	320	51.6	−3.7	5.7	0.11
	20	305.2	–	56.1	0	~0	0
	40	307.7	–	52.3	0	0	0
$T_{c,c}$ = 250 °C, 10 min	5	303	322	40.8	−21.7	28.8	0.71
	10	304	321	52.0	−1.7	3.2	0.06
	20	305	–	49.4	0	0	0
	40	308	–	46.0	0	0	0

Table 3 Relative changes of P_1 and P_2 melting in cold-crystallized PEKm as functions of annealing time. All samples were cold-crystallized at 230 or 250 °C for various times prior to DSC scanning analysis at 10 °C/min

Cold-crystallization	Holding time, (min)	$T_{m,1}$ (°C)	$T_{m,2}$ (°C)	$\Delta H_{f,1}$ (J/g)	$\Delta H_{c,3}$ (J/g)	$\Delta H_{f,2}$ (J/g)	$\Delta H_{f,2}/\Delta H_{f,1}$
$T_{c,c}$ = 230 °C	10	303.9	322	45.4	−9.5	10	0.22
	30	304	322	52.7	−8.1	12.4	0.24
	60	303.6	322	56.8	−13.8	14.6	0.26
$T_{c,c}$ = 250 °C	10	304	321.7	51.2	−2.2	3.0	0.06
	30	304	321.9	48.0	−4.0	5.8	0.12
	60	304	321.6	47.8	−1.9	3.0	0.06

entity at $T_{m,2}$ may be generated with a mechanism of crystal transformation between the P1 and P2 crystals. The details of the mechanism are to be discussed with experimental proof. Although the P1 crystal entity might be formed by crystallization at 230 or 250 °C (or thermal annealing at temperatures below $T_{m,1}$), the P2 entity could be generated only from melting of the P1 crystal entity and recrystallization into P2 (upon scanning to about 308 °C). However, the extent of re-melting/recrystallization depended on the number of thin P1 lamellae available for repacking during the time frame of scanning. For the samples which were annealed at lower temperatures for longer times, the crystal entities would comprise a higher percentage of thin lamellae. The numerical comparison (Tables 2, 3) of the thermal transitions (scanned at the same rates) for the 230 °C- and 250 °C-crystallized samples indicates that the magnitudes of the third crystallization exotherm and second melting peak (P2) are relatively larger for the 230 °C-crystallized samples, but are smaller for 250 °C-crystallized ones.

Interrelation between P1 and P2 crystals

A cold-crystallized PEKm would develop a specific morphology corresponding to the thermal history; however, upon postannealing at higher temperatures a previously cold-crystallized PEKm, its morphology may undergo changes. If melting/recrystallization of P1 and repacking into a P2 crystal was indeed a valid mechanism, it could be expected that isothermal holding at temperatures near the exothermic (recrystallization) peak between P1 and P2 would result in a more significant amount of P2 crystal.

To exactly understand the effect of holding at 300–312 °C on the formation of the P2 crystal entity, a series of samples were first cold-crystallized by heating from quenched amorphous glass and were further postannealed at 312 °C for various periods of time ranging from 0 to 120 min. The samples were then scanned in the DSC from the holding temperature (308 °C) all at the same scanning rate (5 °C/min). The DSC traces are shown in Fig. 6 and the effect of holding time at 308 °C on the amount of repacked P2 crystal that can be generated by melting/recrystallizing the P1 species is compared. Apparently, the P1 crystal was melted immediately to a liquid at 308 °C, but it took time to gradually transform (recrystallize, repack) to a P2 crystal when held at 308 °C. The melting peak of P2 was integrated and compared for these samples. Sample a was scanned from the amorphous glassy state at 5 °C/min, which developed a cold-crystallized morphology with primarily P1 crystals during scanning up to 308 °C. With no holding at 308 °C, sample a was scanned with no interruption, with P1 being melted, and was then repacked into P2 during the short time frame and dynamic heating (5 °C/min) up to 340 °C. The measured $\Delta H_{f,2}$ for the P2 crystal is only 35.3 J/g.

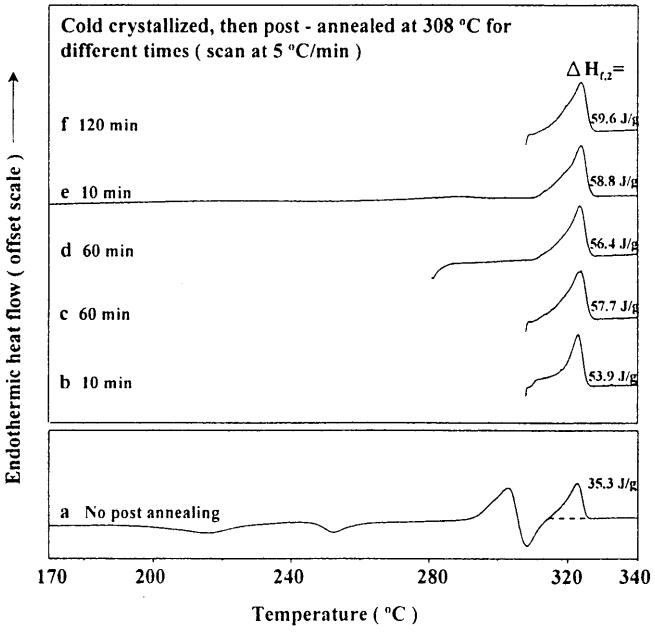

Fig. 6 DSC traces showing the effect of holding time at 308 °C on the amount of repacked P2 crystal that can be generated by melting/recrystallizing the P1 species

Sample b, however, was scanned at 5 °C/min to 308 °C, held there for 10 min, then the scanning (at same rate) was resumed to the final temperature of 340 °C. $\Delta H_{f,2}$ for the P2 crystal in sample b is significantly higher (53.9 J/g) than for sample a. For holding times of 60 and 120 min, the $\Delta H_{f,2}$ for the P2 crystal are even higher, at about 57 and 60 J/g, respectively.

Note that heating a cold-crystallized sample to 308 °C would melt away the P1 crystal entity ($T_{m,1}$), which would then repack into the P2 crystal entity if given sufficient time. It was critical to confirm that once the P1 crystal had melted at 308 °C and repacked fully to a P2 crystal by extended holding at 308 °C, the P1 crystal would not reappear upon cooling the sample. Two special samples (samples d and e) were prepared. After scanning at 5 °C/min to 308 °C, the samples were allowed to stay isothermally at 308 °C for 60 min of time. The results already showed holding at 308 °C for 60 min was sufficient to transform all the initial P1 into the final P2 crystal and reach a maximum crystallinity comprising only the P2 crystal entity. The samples were then quenched from 308 to 280 °C or lower (to preserve the morphology at developed 308 °C). They were both then scanned at 5 °C/min to reveal their thermal transitions in order to reveal the developed morphology. Apparently, both samples revealed no traces of the P1 crystal but only the P2 crystal. No additional crystallization exotherm was found in the DSC traces for these samples, indicating completion of P1 transformation to P2 after they had been held at 308 °C for 60 min or longer. These samples exhibited a measured $\Delta H_{f,2}$ (P2 crystal) which is about the same (56.4 and 58 J/g, respectively) as sample c (holding at 308 °C for 60 min with no quenching to lower temperatures prior to DSC characterization).

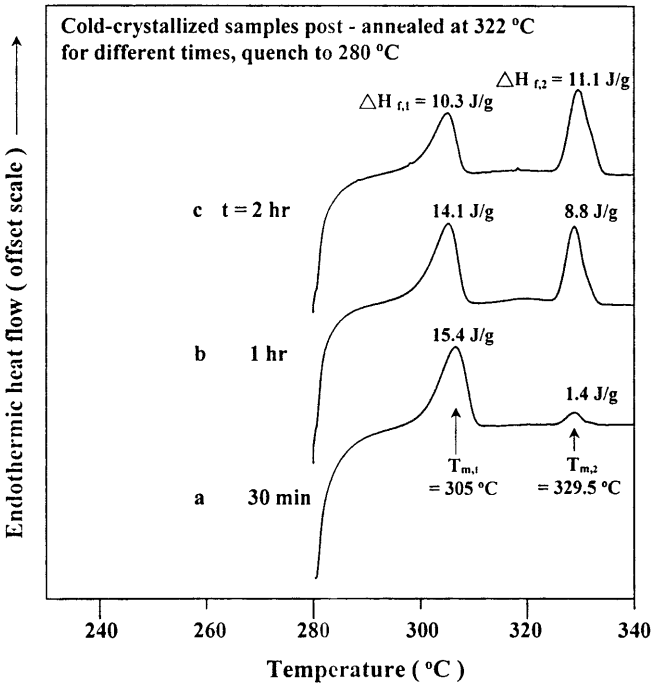

Fig. 7 DSC results (all scanned at 10 °C/min) of three PEKm samples subjected to three different thermal histories

Cold crystallization at $T_{c,3}$

Next, experiments were performed with a higher temperature (322 °C) for cold crystallization, which is at $T_{c,3}$ and close to $T_{m,2}$. The purpose was to understand whether or not a higher annealing temperature would lead to an even higher $T_{m,2}$ and the relationship between the amounts available for packing into crystal entities of $T_{m,1}$ and. $T_{m,2}$. DSC results (all scanned at 10 °C/min) of three PEKm samples subjected to three different thermal histories are shown in Fig. 7. Sample a was prepared by heating a quenched amorphous PEKm to 322 °C, held for 30 min, cooled quickly to 280 °C, then scanned at 10 °C/min from 280 to 340 °C. Sample b was heated to 322 °C, held for 60 min, cooled quickly to 280 °C, then scanned at 10 °C/min from 280 to 340 °C. Sample c was heated to 322 °C, held for 120 min, cooled quickly to 280 °C, then scanned at 10 °C/min from 280 to 340 °C. The DSC traces show that P2 as well as P1 melting is seen in the samples; they were developed at a different times though. The observed crystal entity of P2 in the samples was developed during holding at 322 °C. It is critical to point out here that annealing at 322 °C led to packing of the P2 crystal by melting the previously existing P1; thus, it did not contain any P1 crystal when annealing at 322 °C. Note a higher annealing temperature also led to higher $T_{m,2}$. The $T_{m,2}$ (329 °C) for the P2 crystal in the 322 °C-annealed samples is higher than the 312 °C-annealed samples ($T_{m,2}$ = 321 °C). The melting endotherm ($\Delta H_{f,2}$) for P2 has an increasing magnitude in proportion to the holding time at 322 °C. $\Delta H_{f,2} = 1.4$, 8.8, and 11.1 J/g for holding times of 30, 60, and 120 min (at 322 °C), respectively.

The P1 crystal in the samples was developed upon DSC scanning from 280 °C after the annealing treatments. That is, we have demonstrated that in this designed thermal treatment, the P1 crystal could be intentionally delayed until after the formation of the P2 crystal. The melting endotherm ($\Delta H_{f,1}$) for P1 is higher in samples that have a lower $\Delta H_{f,2}$. The figure shows $\Delta H_{f,1}$ is 15.4, 14.1, and 10.3 J/g (P1), respectively, for the samples whose $\Delta H_{f,2}$ are 1.4, 8.8, and 11.1 J/g (P2) for holding time of 30, 60, and 120 min (at 322 °C), respectively. This suggests that if more crystal species were already packed into the P2 type during 322 °C annealing, there would be less available for packing into the P1 crystal type after it was cooled back from 322 to

280 °C and scanned up. Apparently, if all available polymer species had gone to pack into the high-melting P2 crystal upon annealing at 322 °C, there would have been nothing left to pack into the low-melting P1 crystal upon cooling back to 280 °C and scanning up.

Annealing at 322 °C apparently led to packing of a much thicker P2 crystal, but it proceeded much more slowly than annealing at 312 °C. The amounts of the sum of both crystal entities for the 322 °C-annealed samples are significantly reduced in comparison to those for the 312 °C-annealed ones (compared for the same holding time). The presence of both P1 and P2 in the 322 °C-annealed samples is quite different from what was observed in the 312 °C-annealed samples, which showed only P2 but no trace of P1 upon DSC scanning. Apparently, this could be attributed to the condition that the higher annealing temperature of 322 °C led to a slower rate of packing of the high-melting P2 crystal entity (though further elevated); thus, some melted crystallizable polymer chains were still available for repacking into crystals upon scanning within the lower temperature range. The reappearance of the P1 endotherm in these samples indicates that although the crystal entity of $T_{m,1}$ was melted away upon heating/holding to 322 °C, the P1 crystal could be repacked during scanning from 280 °C as long as there were still amorphous polymer chains available. Note that the newly repacked P1 crystal no longer melted and repacked into P2 upon scanning. This is indicated by the absence of a crystallization exotherm between P1 and P2. This suggests that the repacked crystal entity of P1 may be of a thicker lamellar type, and it can simply melt but does not recrystallize in time to repack to P2 upon scanning in the DSC at 10 °C/min.

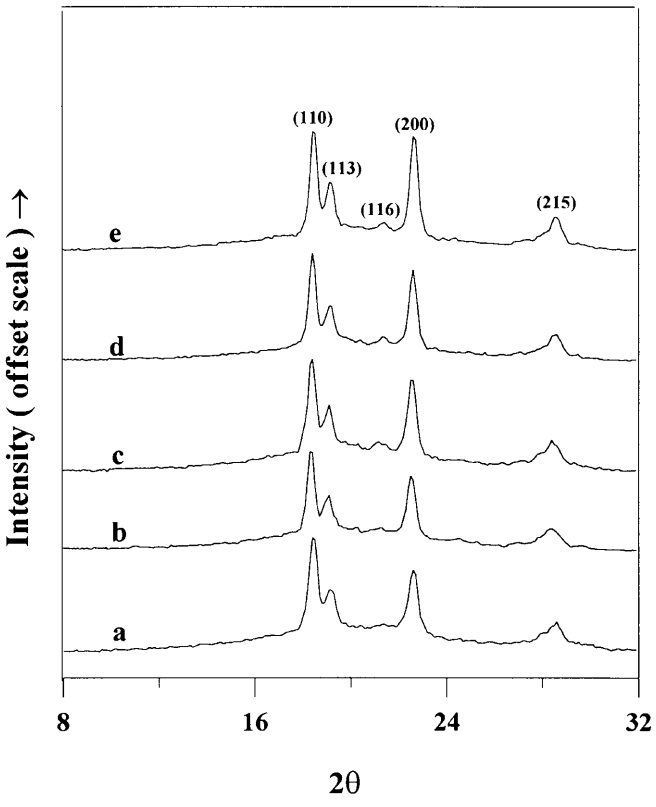

Fig. 8 X-ray diffractograms for PEKm cold-crystallized by heating from an initially amorphous state at 5 °C/min to 290 °C then quenched to ambient temperatures to preserve its developed morphology (*a*), 10 °C/min to 290 °C then quenched (*b*), 5 °C/min to 307 °C then quenched (*c*), 5 °C/min to 307 °C for 15 min then quenched (*d*)

Crystal/morphology analysis

To discern the unit-cell packing, the samples were examined using X-ray diffraction. X-ray diffractograms for PEKm samples cold-crystallized by dynamic heating from the initially amorphous state are shown in Fig. 8. Note that samples a and b would have exhibited dual melting peaks if they had been scanned directly from 290 °C. That is, they both contained crystal entities that yielded $T_{m,1}$ and $T_{m,2}$. Sample c would have melted its crystal entity associated with $T_{m,1}$, but would exhibit the second melting peak (P2) if scanned from 307 °C. Sample d was similar to sample c in that it contained only the crystal entity of $T_{m,2}$, except that the crystal entity associated with $T_{m,2}$ would be present in a larger quantity owing to the additional isothermal holding at 307 °C before quenching to ambient temperature. It is clear that these four samples are different in melting behavior; however, all the samples showed four major diffraction peaks (for 110,113, 200, and 215 planes) at exactly the same angles and these are in agreement with the values reported in the literature for PEKm [2]. Thus, most likely, the crystal species showing multiple (dual) melting are related to lamellar thickness and types. Further analysis was also performed to understand if there was any difference in the crystal unit cells produced in the two crystallization processes (at $T_{c,1}$ and $T_{c,2}$). For simplicity, the wide-angle X-ray diffraction diffractograms are similar to Fig. 8 and not shown here. Sample a was subjected only to the first crystallization process (at $T_{c,1} =$ 230 °C), while sample b was subjected to both the first and second crystallization processes (whose peaks are $T_{c,1} = 230$ °C and $T_{c,2} = 250$ °C, respectively). Four diffraction planes were identified, (110), (113), (200), and (215), which are identical for both samples, suggesting that the crystal entities packed in these two crystallization processes are the same in terms of crystal unit cell (orthorhombic). This result is different from those reported by Blundell et al. [3] and Rueda

and Zolotukhin [13], who concluded that dramatic changes with respect to temperature in the crystal unit cell dimensions in melt-processed PEKm or an oligo (aryl ether ketone) took place.

The lamellar perfection or thickness developed in these two-cold crystallization processes, however, might be different. Changes in the spherulite/lamellae morphologies at different temperatures of cold crystallization were examined using polarized optical microscopy. The spherulite morphology of cold-crystallized PEKm is shown in Fig. 9 at different temperatures. When cold-crystallized at low temperatures (260 °C or lower), PEKm developed typical Maltese cross spherulites containing primarily P1 lamellae (graph a). With the temperatures increasing to 280 °C, some preliminary melting/reorganization took place and the lamellae were thickened to assume a sheaflike pattern (graph b). When PEKm was heated to and cold-crystallized at a higher temperature of 300 °C, dramatic melting of previously formed spherulites took place, leaving only tiny crystal cores of higher melting species (graph d). Finally, when held at 310 °C, the melted species were reorganized into thicker lamellae of P2 species (graph e).

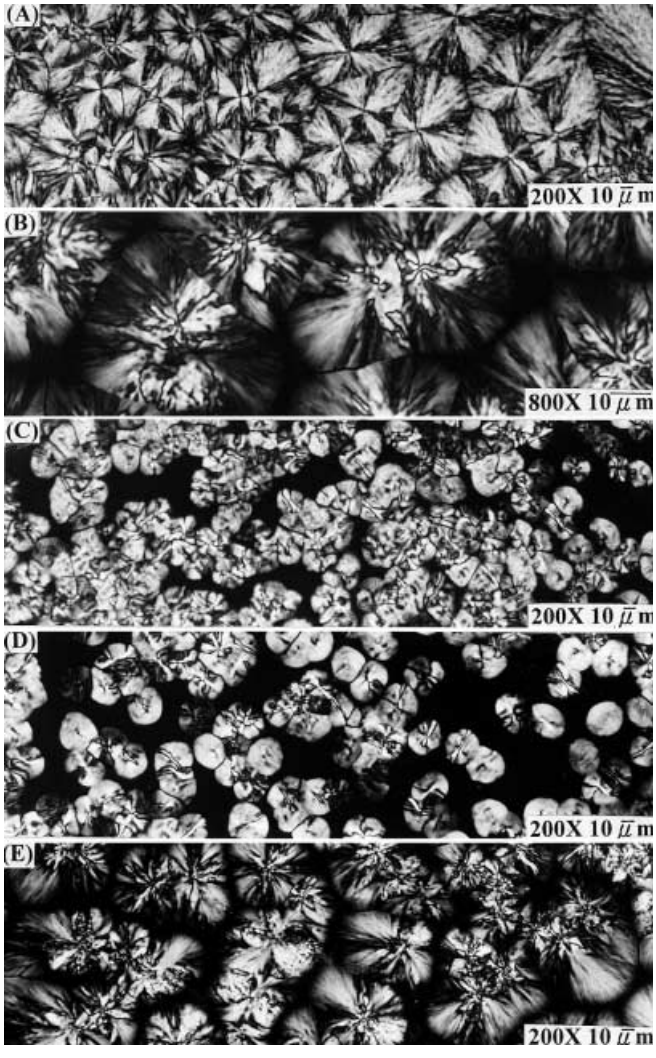

Fig. 9 Polarized optical microscopy images showing the spherulite morphology of cold-crystallized PEKm at different temperatures: **a** 260, **b** 280, **c** 290, **d** 300, and **e** 310 °C

Conclusion

By focusing on cold-crystallized PEKm, this study yielded a critical clue that both preexisting dual lamellae and reorganization upon heat-scanning/annealing may be responsible for the multiple melting phenomenon commonly seen in semicrystalline polymers. A concurrent work on melt-crystallization features of PEKm also revealed additional evidence supporting the mechanisms discussed. This study has shed new light on the interpretation of multiple melting with respect to relationships between polymorphism and melting in polymers. When PEKm was cold-crystallized, only the lower-melting P1 crystal entity ($T_{m,1} \sim 300$ °C), and no higher-melting P2 crystal, was present and appeared as small spherulites. The thicker P2 crystal ($T_{m,2} \sim 320$ °C), however, can be generated during heating scans or annealing previously cold crystallized PEKm. The melting behavior and thelamellar and spherulitic morphology differed significantly in PEKm subjected to cold crystallization at $T_{c,1}$, $T_{c,2}$, or $T_{c,3}$. However, the crystal cell (orthorhombic with the same a, b, c) is identical regardless of the temperature of the cold crystallization. The same multiple melting phenomenon can be observed in a semicrystalline polymer that contains either (a) a single original crystal (lamella), or (b) two (or more) preexisting crystal (lamellae) types. In case a, the multiple melting can be attributed to the melting of the original crystal and repacking to another crystal. In case b, however, the multiple melting was indeed an indication of two or more originally coexisting different lamellae in the polymer. To discriminate between these two mechanisms, it is critical to examine the morphology of the polymers. This study has confirmed routes via repacking of higher-melting crystals by melting/recrystallizing previously existing lower-melting crystals. In addition, multiple-melting phenomenon could also be attributed to coexisting dual crystals/lamellae.

Acknowledgement This work was supported by the National Science Council of Taiwan, to which the authors express their sincerest gratitude. Grant numbers: NSC 87 2216 E006 005 and NSC 89 2216 E006 014.

References

1. Cheng SZD, Ho RM (1996) Macromol Chem Phys 197:185–213
2. Blundell DJ, Liggat JJ, Flory A (1992) Polymer 33:2475–2482
3. Zolotukhin MG, Rueda D, Andre I, Ripoll MM, Abajo JD, Alvarez JC (1997) Macromol Chem Phys 198: 2089–2099
4. Wunderlich B (1976) Macromolecular physics, vol 1. Academic, New York
5. Blundell DJ (1987) Polymer 28:2248–2251
6. Lee Y, Porter RS (1987) Macromolecules 20:1336–1341
7. Ko TK, Woo EM (1996) Polymer 37: 1167–1175
8. Ho RM, Cheng SZD, Hsiao SB, Gardner KH (1995) Macromolecules 28: 1938–1945
9. Marand H, Prasad A (1992) Macromolecules 25:1731–1736
10. Sun YS, Woo EM (1999) Macromolecules 32:7836–7844
11. Zolotukhin MG, Rueda D, Andre I, Ripoll MM, Abajo DJ, Alvarez JC (1997) Macromol Chem Phys 198: 2089–2099
12. Rueda DR, Garcia MC, Gutierrez AF, Zolotukhin MG, Balta Calleja FJ (1998) Macromolecules 31:8201–8208
13. Rueda DR, Zolotukhin MG (1997) Macromol Chem Phys 198:3517–3528
14. Wang S, Wang J, Zhang H, Wu Z, Mo Z (1996) Macromol Chem Phys 197: 1643–1650
15. Liggat JJ, Staniland PA (1991) Polym Commun 32:450–452